Published in final edited form as:
Radiology. 2014 July ; 272(1): 241–251. doi:10.1148/radiol.14131603.

Three-Station 3D Bolus Chase MR Angiography Using Real-Time Fluoroscopic Tracking

Casey P. Johnson, Ph.D.[1], **Paul T. Weavers, B.S.**[2], **Eric A. Borisch, M.S.**[2], **Roger C. Grimm, M.S.**[2], **Thomas C. Hulshizer, B.S.**[2], **Christine C. LaPlante, M.S.**[2], **Phillip J. Rossman, M.S.**[2], **James F. Glockner, M.D., Ph.D.**[2], **Phillip M. Young, M.D.**[2], and **Stephen J. Riederer, Ph.D.**[2]

[1]Department of Radiology, University of Iowa, Iowa City, IA

[2]MR Research Laboratory and Department of Radiology, Mayo Clinic, Rochester, MN

Abstract

Purpose—To perform a preliminary clinical feasibility study of the real-time fluoroscopic tracking technique for bolus chase MR angiography (MRA) of peripheral vasculature to image three stations extending from the aortoiliac bifurcation to the pedal arteries.

Materials and Methods—21 subjects comprised of eight healthy volunteers (3 male; mean age: 48 yr; age range: 30–81 yr) and 13 patients with suspected peripheral arterial disease (5 male; mean age: 67 yr; age range: 47–81 yr) were enrolled in an IRB-approved and HIPAA-compliant prospective study and provided informed consent. All subjects were imaged with the fluoroscopic tracking MRA protocol. Ten patients were additionally imaged with a clinical CT angiography (CTA) runoff exam. Two readers scored the MRA studies for vessel signal and sharpness and presence of confounding artifact and venous contamination at 35 arterial segments. Mean aggregate scores were assessed. The paired MRA and CTA studies were additionally scored for visualization of disease, reading confidence, and overall diagnostic quality and compared using a Wilcoxon signed rank test.

Results—Real-time fluoroscopic tracking performed well technically in all studies. Vessel segments were scored good to excellent in all evaluation categories with the following exceptions: for vessel signal and sharpness, the abdominal aorta, iliac arteries, distal plantar arteries, and plantar arch were scored fair to good; and for presence of confounding artifact, the abdominal aorta and iliac arteries were scored fair. The MRA and CTA studies did not differ significantly in any scoring category (Reader 1: p=0.50, 0.39, and 0.39; Reader 2: p=0.41, 0.61, 0.33). CTA tended to be favored overall as it was scored “substantially better” in 20% (4/20) and 25% (5/20) of the pooled evaluations for the visualization of disease and overall image quality categories, respectively, versus 5% (1/20) for MRA in both categories.

Conclusion—Three-station bolus chase MRA using real-time fluoroscopic tracking provided high-spatial-resolution arteriograms of the peripheral vasculature, enabled precise triggering of table motion, and compared well to CTA.

Corresponding Author: Stephen J. Riederer, Ph.D., 200 First St SW, Rochester, MN 55905, Tel: 507-284-6209, Fax: 507-284-9778, riederer@mayo.edu.

This manuscript has not been presented at an RSNA meeting nor has it been accepted for presentation at a future meeting.

INTRODUCTION

Bolus chase contrast-enhanced MR angiography (CE-MRA) is commonly used to image peripheral arterial disease over the extent of the lower extremities. Since its introduction 15 years ago (1, 2), bolus chase MRA has continued to evolve, with technical advancements that have improved imaging efficiency, spatiotemporal resolution, and acquisition timing. Current techniques employ station-specific imaging parameters (3), parallel imaging with acceleration as high as R=4 (4, 5), patient-specific and physiologically-based imaging parameters (6), and often hybrid techniques to acquire a time-resolved acquisition at the distal-most station prior to the bolus chase runoff (7, 8). These and other technical developments have made bolus chase MRA a competitive alternative to other modalities such as computed tomography angiography (CTA) and digital subtraction angiography (DSA) (9–11).

Bolus chase MRA can continue to benefit from technical advancements to address a number of limitations. First, current techniques typically rely on two or more injections of contrast material to estimate the contrast bolus transit time or allow multiple phases of arterial imaging, which adds time, complexity, and possible contrast material dose to the imaging protocol. Second, spatiotemporal resolution is often limited to reduce proximal station dwell times to keep pace with the progressing contrast bolus. Third, fixed imaging parameters and timing protocols are often used and cannot be easily adapted to efficiently account for patient-specific hemodynamics.

A recently described approach to bolus chase MRA called fluoroscopic tracking can potentially address these limitations. Fluoroscopic tracking has been demonstrated for dual-station imaging of the thighs and calves (12) and calves and feet (13). In these feasibility studies, high image acceleration (R_{net}>14) and view sharing were applied to acquire 3D angiograms at two imaging stations with both high spatial (≤1.0 mm^3) and high temporal (2.5 to 6.7 sec frame time) resolution. Additionally, 3D time frames at the proximal station were reconstructed in realtime, enabling visual tracking of the arrival and progression of the contrast bolus and manual triggering of table advance to the distal station. The method allows imaging following a single injection of contrast material, without prior knowledge of patient hemodynamics or contrast bolus transit times, and nominal spatiotemporal resolution observed is competitive with single-station CE-MRA methods.

The purpose of this study was to perform a preliminary clinical feasibility study of the real-time fluoroscopic tracking technique for bolus chase MRA of peripheral vasculature to image three stations extending from the aortoiliac bifurcation to the pedal arteries.

MATERIALS AND METHODS

Fluoroscopic Tracking Technique

Fluoroscopic tracking aims to image proximal stations with sufficient spatial and temporal resolution to acquire diagnostic-quality 3D angiograms, enable real-time assessment of contrast bolus progression, and avoid venous contamination at the distal-most station. To accomplish this for three-station imaging, the proximal abdomen-pelvis and thigh stations

were imaged with the following technical specifications: (i) 2.5 sec frame time to allow precise tracking of the contrast bolus; (ii) 1.5 mm isotropic spatial resolution for accurate diagnosis; (iii) <7 sec temporal footprint to rapidly build up image quality (14) and enable a short station dwell time (<10 sec) to quickly chase the contrast bolus down the periphery; and (iv) <250 ms latency of reconstructed time frames to provide sufficient time for the operator to trigger table motion. The distal-most calf-foot station was imaged with 1.0 mm isotropic spatial resolution and frame time relaxed to 5.2 sec. Note that the spatial resolution of the proximal stations need not be as fine as the calf-foot station due to larger vessel size, allowing for higher real-time temporal resolution.

To achieve these technical performance targets, spatial and temporal resolution were carefully traded off using a highly-accelerated acquisition strategy (Figure 1). The Cartesian acquisition with projection reconstruction-like sampling (CAPR) technique (15) was used in combination with R=8 2D sensitivity encoding (SENSE) (16) and R=1.9 2D partial Fourier acceleration to rapidly update time frames and build up image quality via view sharing with a short temporal footprint (14). The fluoroscopic tracking method has been outlined previously for two-station imaging (12) and consists of data collection using multiple receiver arrays, feeding of raw data to a custom reconstruction server, real-time display of reconstructed 3D time frame maximum-intensity projections (MIPs) on a graphical user interface, and operator-triggered table motion via feedback to the imaging system. A similar arrangement was used in this study with real-time processing at two proximal stations.

Subjects

The study was approved by the Institutional Review Board, and each participant provided written informed consent. Eight healthy volunteers and 13 patients with suspected peripheral arterial disease participated in this prospective Health Insurance Portability and Accountability Act (HIPAA) compliant study between October 2011 and December 2012. Three of the healthy subjects were male (mean age = 57 yr; range = 44–81 yr) and five were female (mean age = 43 yr; range = 30–53 yr). Of the patients, five were male (mean age = 77 yr; range = 72–81 yr) and eight were female (mean age = 61 yr; range = 47–79 yr). All subjects underwent a three-station contrast-enhanced MRA exam using the fluoroscopic tracking technique described above. The healthy volunteers and ten of the patients were recruited, whereas the other three patients were referred clinically for the MRA technique. The ten recruited patients (four male and six female) were additionally imaged with bolus chase CTA at most one day prior to the MRA, which is the standard clinical runoff protocol at our institution. These patients were scheduled for a clinical CTA exam with an indication for peripheral arterial disease at the time of recruitment. Recruitment was only attempted if the MRI system on which the fluoroscopic tracking protocol was implemented was available within one day of the CTA exam. To be included in the study participants needed to be at least 18 years old. Study exclusion criteria, including the number of subjects excluded for each criterion, were: metal in body – 6; allergy to contrast agent – 3; claustrophobia – 3; estimated glomerular filtration rate (eGFR) <30 mL/min/1.73m^2 – 4; pregnancy or breast feeding – 0; and scheduling conflicts – 12. Qualitative results for five healthy volunteer studies have been previously reported in a conference abstract (17).

MRA Imaging Protocol

Subjects were imaged at three stations (abdomen-pelvis, thigh, and calf-foot), each providing 42 cm of superior/inferior (S/I) coverage, using a 3T MRI system (Discovery MR750; GE Healthcare; Waukesha, WI). The extended longitudinal field-of-view (FOV) was 122 cm after two 40 cm table moves. A custom-built 32-channel modular receiver coil array was used to provide high parallel imaging performance at each station. The array consisted of 16 pairs of identically-shaped rectangular elements (length: 40 cm; width: 13 cm) that could be flexibly combined to fit a variety of body types. In this study, 12, 10, and 8 coil elements were typically used at the abdomen-pelvis, thigh, and calf-foot stations, respectively, to provide a close fit to the body. At each station the elements were configured in a linear array and then wrapped circumferentially around the patient. Prior to securing the receiver arrays at each station, the subject's legs were wrapped in a sheet to minimize motion and the feet were wrapped in a warm blanket to promote vasodilation for improved visibility of the pedal arteries. The three-station imaging protocol consisted of the following steps: (i) scout acquisitions; (ii) volume prescriptions and prescanning; (iii) calibration acquisitions for SENSE unfolding; (iv) real-time system initialization and calculation of SENSE inversion matrices; (v) subtraction mask acquisitions; (vi) contrast material injection; and (vii) time-resolved bolus chase runoff acquisition with fluoroscopic tracking providing real-time triggering of table advance. This protocol typically required 15 minutes to complete all three stations. Patients were instructed to breathe shallowly while imaging the abdomen-pelvis station to reduce respiratory motion.

Station-specific imaging parameters for the 3D time-resolved bolus chase MRA acquisition with fluoroscopic tracking are listed in Table 1. The delay time to switch between stations was 5.0 sec, which included time to close the station sequence after completing the acquisition (1.0 sec), physically move the table (3.0 sec), load the next station sequence (0.65 sec), and play out dummy repetitions to reach a sufficient steady state signal for reliable subtraction (0.35 sec). Receiver array coils were dynamically switched such that only coils at the imaging station were sampled. Intravenous administration of a single dose of contrast material by power injector (Spectris Solaris; Medrad Inc; Indianola, PA) consisted of 8–20 mL (mean dose: 0.14 mmol/kg; range: 0.08–0.20 mmol/kg) of gadobenate dimeglumine (MultiHance; Bracco Diagnostics; Princeton, NJ) followed by 20 mL of saline flush injected at a rate of 2–3 mL/sec. The volume of administered contrast material was determined based on an individual's eGFR measured in units of mL/min/1.73m^2. A standard volume of 20 mL was administered if eGFR was >60. If eGFR was <60, then the volume was reduced to yield a dose of 0.08 mmol/kg. For display, proximal station angiograms were interpolated to 1.0 mm isotropic resolution to match the calf-foot station resolution.

CTA Imaging Protocol

CTA was performed using a dual-source CT system (Definition; Siemens; Erlangen, Germany) with 128 × 0.6 mm detector configuration, 0.5 sec rotation time, and 0.4 pitch. Source peak voltage and current were 120 kVp and 250 mA, and automated tube current modulation was employed. Iohexol contrast agent (Omnipaque 350; GE Healthcare; Waukesha, WI) was administered via power injector in a rate-based split injection algorithm (first dose 20–30 mL at 4–6 mL/sec, second dose 95–140 mL at 3–4 mL/sec) followed by 30

mL saline flush at 3–4 mL/sec. Automated triggering was employed. Images were reconstructed with 0.6 × 0.6 mm^2 in-plane resolution and 2.0 mm S/I slice thickness at 1.2 mm intervals. Anatomic coverage extended either from the top of the diaphragm (XX patients) or the crest of the ilium (XX patients) down through the toes depending on patient size. Following the first run, a second run was immediately performed from the knees to the toes in patients over the age of 50 in case the first run outstripped the contrast bolus.

Image Quality Assessment

Angiogram image quality was independently evaluated in two parts by two radiologists specializing in body MRI and CT with 16 and 4 years of experience (JFG and PMY). The readers had access to all source images of the MRA and CTA exams including the time series volumes. Evaluations were performed using GE Healthcare AW Workstation (Waukesha, WI) and TeraRecon (Foster City, CA) software. In the first part, the N=21 MRA studies were scored in four image quality categories: (i) vessel signal; (ii) vessel sharpness; (iii) presence of confounding artifact; and (iv) presence of confounding venous contamination. 17 arterial segments were scored bilaterally as well as the distal abdominal aorta (35 segments total) on a scale of 1 to 5 (1 = poor; 2 = marginal; 3 = fair; 4 = good; and 5 = excellent). No score was given in cases where an arterial segment was not seen (e.g., due to disease or being positioned outside of the FOV). In the second part, the N=10 companion MRA and CTA angiograms were scored pairwise in three categories: (i) visualization of disease; (ii) reading confidence; and (iii) overall diagnostic quality. Scores were given on a ranked scale of −2 to +2 (−2 = MRA substantially better; −1 = MRA marginally better; 0 = neutral; +1 = CTA marginally better; and +2 = CTA substantially better).

Bolus Timing Assessment

For all MRA studies, the times at which the contrast bolus was first observed (detection time), the contrast bolus was observed to reach the distal end of the station FOV in both legs (traversal time), and table motion was initiated to the subsequent station (trigger time) were recorded at both proximal stations. From these measurements, the station dwell (trigger minus detection), bolus transit (traversal minus detection), and the trigger delay (trigger minus traversal) times were calculated. The contrast bolus progression was considered “rapid” if the bolus transit times at the abdomen-pelvis and thigh stations were less than 5 and 2.5 sec, respectively, and “slow” if the times were greater than 5 and 2.5 sec, respectively.

Statistical Analysis

The mean and standard deviation of reader aggregate vessel segment scores for each image quality category were separately calculated for the eight healthy volunteer and 13 patient studies. Scores for each leg were combined in the averages. To determine if either reader scored the MRA or CTA studies more favorably in each comparison category, a Wilcoxon signed rank test was used with a significance threshold of α=0.05 and estimated power of 0.8. This calculation was performed using the R software environment (version 3.0.1; R Foundation for Statistical Computing; Vienna, Austria).

RESULTS

Average image quality assessment scores for each arterial segment are tabulated in Table 2. Two of the segments, the distal plantar and plantar arch, were often outside of the imaging FOV and thus did not receive as many scores. For vessel signal and sharpness, the lowest scoring segments were the abdominal aorta, iliac arteries, distal plantar arteries, and plantar arch, with scores ranging from fair to good. All other segments were scored good to excellent. For presence of confounding artifact, the abdominal aorta and iliac arteries had the lowest scores and were reported as fair. These artifacts are attributed to imperfect subtractions and SENSE-related noise amplification and aliasing, which was most pronounced at the abdomen-pelvis station due to the presence of motion and the anatomy filling nearly all of the FOV. All other vessel segments were scored as good. For presence of confounding venous contamination, all vessel segments received scores of good to excellent. In all categories, the healthy volunteer studies typically scored better than the patient studies. The greatest difference was in the venous contamination scores at the calf-foot station. Seven of the patient studies had rapid arterial-to-venous transit, which resulted in average scores of good as opposed to excellent for segments distal to the tibioperoneal trunk. Patient scores were lower in the other three categories mostly due to the presence of disease (e.g., rapid arterial-to-venous transit, stent artifacts, and complex vasculature and flow). One patient study had particularly poor image quality due to gross motion-related artifact at all three stations.

No statistically significant differences were observed between the paired MRA and CTA comparisons (Table 3). CTA tended to be favored overall as it was scored “substantially better” in 20% (4/20) and 25% (5/20) of the pooled evaluations for the visualization of disease and overall image quality categories, respectively, versus 5% (1/20) for MRA in both categories. This analysis includes Subject 18, for whom the CTA was scored “substantially better” by both readers in all three categories due to severe motion artifacts in the MRA. In general, MRA was preferred in cases with slower contrast bolus progression and arterial-to-venous transit, whereas CTA was preferred in cases where the MRA had artifacts due to motion, acceleration, or stents or venous contamination due to rapid arterial-to-venous transit.

For all 21 cases, the fluoroscopic tracking technique was technically successful in that the contrast bolus was successfully imaged at both proximal stations in real-time and table advance was successfully triggered by the operator. Bolus timing assessment results are shown in Figure 2 and Table 4. Broad ranges of bolus detection and transit times were accommodated. In most cases, the contrast bolus had already traversed the thigh station by the time the table had moved to this station. Therefore, the dwell time at this station was typically limited to only 5.0 sec or two time frames. Despite this short dwell time, image quality at this station was typically good (Table 2). The trigger delay times were usually 5.0 sec at both stations, which corresponds to triggering the table when the bolus traversed the station FOV.

Representative angiograms acquired using fluoroscopic tracking are shown in Figures 3–6 (also see companion Supplemental Movies 1–4, respectively, for 3D temporal dynamics).

For most healthy volunteers, only two time frames were acquired at the thigh station. Despite a resultant short 5.0 sec dwell time at this station, image quality was typically good to excellent and venous contamination was routinely avoided at the calf-foot station (Figure 3 and Supplemental Figure 1). In patients with slow contrast bolus progression, fluoroscopic tracking enabled observation of contrast bolus progression through both proximal stations and lead to high image quality throughout the extended FOV (Figure 4). In patients with rapid contrast bolus progression, the thigh station dwell time was limited to 5.0 sec, which helped avoid degrading venous contamination (Figure 5). Cases where the MRA exam did not score as well typically included artifact at the abdomen-pelvis station and/or rapid arterial-to-venous transit at the calf-foot station (Figure 6).

DISCUSSION

Fluoroscopic tracking enabled high-spatial-resolution imaging from the aortoiliac bifurcation to the pedal arteries and flexibly accommodated a broad range of subject hemodynamics. The acquired spatiotemporal resolution at the proximal stations (1.5 mm isotropic and <7 sec temporal footprint) is competitive with if not superior to current non-time-resolved bolus chase MRA protocols, which use voxel volumes of 3.8 to 6.6 mm^3 (1.6 to 1.9 mm isotropic) and station dwell times of 8 to 20 sec at the proximal stations (5, 18–21). The method was technically successful in all studies in that the contrast bolus was consistently tracked effectively and efficiently. Arterial segments were typically scored as being of good quality, and in those cases in which it occurred, artifact and venous contamination generally did not interfere with diagnosis. However, one of the studies was severely compromised by patient motion. Promisingly, fluoroscopic tracking performed well compared to CTA. Favorable scoring seemed to follow where disease was present, with MRA typically being advantageous for more distal disease and CTA being advantageous for proximal disease and where stents were located. The first of these is consistent with previous work directly comparing CE-MRA and CTA in imaging of the calves (22). Motion and acceleration artifacts at the abdomen-pelvis station and venous contamination at the calf-foot station in cases of rapid arterial-to-venous transit are the prime issues that next need to be addressed.

The principal advantage of fluoroscopic tracking is its ability to not only track the contrast bolus but also to simultaneously provide efficient imaging at each station. If the contrast bolus is moving quickly, then the fluoroscopic tracking sequence can allow movement of the table in as little as 5.0 sec upon arrival of the contrast bolus to the station FOV while still building up high image quality. Alternatively, if the contrast bolus is moving slowly, then the technique can continue to improve image quality with a more extended imaging duration and provide multiple time frames at that station. Thus, the technique provides an efficient tradeoff of image quality and station dwell time. A second advantage is that only a single injection of contrast material is utilized, obviating need of a timing bolus or hybrid technique. This saves time, simplifies the imaging protocol, and reduces opportunities for timing errors. A third advantage is that the use of high image acceleration (R_{net}>14 at all imaging stations) enables higher nominal spatial resolution and shorter station dwell times than are typical of most bolus chase MRA protocols. Despite the accompanying intrinsic reduction in SNR due to the high acceleration factors, good image quality was still acquired

as evidenced by the fine detail seen in the angiograms and the good assessment scores for both vessel signal and sharpness. We attribute this to the high performance of the circumferentially-placed coil arrays (23) at each station as well as the intrinsic SNR retention when acceleration is applied to CE-MRA (24, 25).

The fluoroscopic tracking methodology can potentially be improved in several ways. First, additional techniques for better retention of SNR at the high two-dimensional acceleration factors could be incorporated, including controlled aliasing in parallel imaging results in higher acceleration (CAIPIRINHA) (26), compressive sensing (27, 28), acceleration apportionment (29), and vascular masking (30). Second, although the technique generally provided good venous suppression at the distal-most station, this would be improved by reduction of the 5.0 sec move time from one station to the next by eliminating software-related overhead and playing out dummy repetitions while the table moves. It may also be possible to acquire data while the table moves (31, 32). Alternatively, in cases that are expected to have rapid arterial-to-venous transit, a targeted time-resolved acquisition at the calf-foot station prior to or after the bolus chase runoff could be performed, as is done with hybrid MRA acquisitions. Third, motion-related artifacts can potentially be addressed using a two-point Dixon technique for subtractionless MRA (33). Another option is to use a blood pool contrast agent, which would enable a quick steady-state acquisition at the abdomen-pelvis station following the first-pass run if needed (34). Lastly, contrast material dose can potentially be further reduced. Good time-resolved calf MRA image quality has been shown with doses of only 0.03 mmol/kg (8). Additionally, given that the station dwell times were short (typically <10 sec), a good fraction of the time the contrast bolus is present in the arteries at a station is likely not being utilized by the fluoroscopic tracking technique, and a shorter, more compact bolus could prove advantageous.

The main limitation of this preliminary study was the number of clinical studies performed. Although the patient population was diverse in terms of disease manifestations and hemodynamics, more studies are needed to evaluate the effectiveness of fluoroscopic tracking-based MRA versus CTA and other MRA methods. In particular, the study had marginal statistical power to determine if the MRA and CTA results were significantly different. Other limitations include individual variation in contrast material dose, inherent bias in the pairwise evaluation of the MRA and CTA studies, and lack of a comparison to a standard clinical MRA or DSA protocol.

In conclusion, three-station bolus chase MRA using fluoroscopic tracking provides high-spatial-resolution arteriograms along the extent of the peripheral vasculature, enables patient-specific triggering of table motion, and is a promising alternative to contemporary MRA and CTA methods.

Supplementary Material

Refer to Web version on PubMed Central for supplementary material.

Acknowledgments

Funding: NIH grants EB000212, HL070620, and RR018898

REFERENCES

1. Ho KY, Leiner T, de Haan MW, Kessels AG, Kitslaar PJ, van Engelshoven JM. Peripheral vascular tree stenoses: evaluation with moving-bed infusion-tracking MR angiography. Radiology. 1998; 206(3):683–692. [PubMed: 9494486]
2. Meaney JF, Ridgway JP, Chakraverty S, et al. Stepping-table gadolinium-enhanced digital subtraction MR angiography of the aorta and lower extremity arteries: preliminary experience. Radiology. 1999; 211(1):59–67. [PubMed: 10189454]
3. Leiner T, Ho KY, Nelemans PJ, de Haan MW, van Engelshoven JM. Three-dimensional contrast-enhanced moving-bed infusion-tracking (MoBI-track) peripheral MR angiography with flexible choice of imaging parameters for each field of view. J Magn Reson Imaging. 2000; 11(4):368–377. [PubMed: 10767065]
4. de Vries M, Nijenhuis RJ, Hoogeveen RM, de Haan MW, van Engelshoven JM, Leiner T. Contrast-enhanced peripheral MR angiography using SENSE in multiple stations: feasibility study. J Magn Reson Imaging. 2005; 21(1):37–45. [PubMed: 15611941]
5. Maki JH, Wang M, Wilson GJ, Shutske MG, Leiner T. Highly accelerated first-pass contrast-enhanced magnetic resonance angiography of the peripheral vasculature: comparison of gadofosveset trisodium with gadopentetate dimeglumine contrast agents. J Magn Reson Imaging. 2009; 30(5):1085–1092. [PubMed: 19856442]
6. Potthast S, Wilson GJ, Wang MS, Maki JH. Peripheral moving-table contrast-enhanced magnetic resonance angiography (CE-MRA) using a prototype 18-channel peripheral vascular coil and scanning parameters optimized to the patient's individual hemodynamics. J Magn Reson Imaging. 2009; 29(5):1106–1115. [PubMed: 19388111]
7. Berg F, Bangard C, Bovenschulte H, et al. Hybrid contrast-enhanced MR angiography of pelvic and lower extremity vasculature at 3.0 T: initial experience. Eur J Radiol. 2009; 70(1):170–176. [PubMed: 18243622]
8. Attenberger UI, Haneder S, Morelli JN, Diehl SJ, Schoenberg SO, Michaely HJ. Peripheral arterial occlusive disease: evaluation of a high spatial and temporal resolution 3-T MR protocol with a low total dose of gadolinium versus conventional angiography. Radiology. 2010; 257(3):879–887. [PubMed: 20959539]
9. Ouwendijk R, de Vries M, Pattynama PM, et al. Imaging peripheral arterial disease: a randomized controlled trial comparing contrast-enhanced MR angiography and multi-detector row CT angiography. Radiology. 2005; 236(3):1094–1103. [PubMed: 16020559]
10. Berg F, Bangard C, Bovenschulte H, et al. Feasibility of peripheral contrast-enhanced magnetic resonance angiography at 3.0 Tesla with a hybrid technique: comparison with digital subtraction angiography. Invest Radiol. 2008; 43(9):642–649. [PubMed: 18708858]
11. Burbelko M, Augsten M, Kalinowski MO, Heverhagen JT. Comparison of contrast-enhanced multi-station MR angiography and digital subtraction angiography of the lower extremity arterial disease. J Magn Reson Imaging. 2013; 37(6):1427–1435. [PubMed: 23188773]
12. Johnson CP, Haider CR, Borisch EA, Glockner JF, Riederer SJ. Time-resolved bolus-chase MR angiography with real-time triggering of table motion. Magn Reson Med. 2010; 64(3):629–637. [PubMed: 20597121]
13. Johnson CP, Borisch EA, Glockner JF, Young PM, Riederer SJ. Time-resolved dual-station calf-foot three-dimensional bolus chase MR angiography with fluoroscopic tracking. J Magn Reson Imaging. 2012; 36(5):1168–1178. [PubMed: 22753021]
14. Johnson CP, Polley TW, Glockner JF, Young PM, Riederer SJ. Buildup of image quality in view-shared time-resolved 3D CE-MRA. Magn Reson Med. 2013; 70(2):348–357. [PubMed: 22936574]
15. Haider CR, Hu HH, Campeau NG, Huston J 3rd, Riederer SJ. 3D high temporal and spatial resolution contrast-enhanced MR angiography of the whole brain. Magn Reson Med. 2008; 60(3): 749–760. [PubMed: 18727101]
16. Weiger M, Pruessmann KP, Boesiger P. 2D SENSE for faster 3D MRI. MAGMA. 2002; 14(1):10–19. [PubMed: 11796248]

17. Johnson, CP.; Borisch, EA.; Rossman, PJ., et al. Three-station time-resolved 3D bolus chase MRA with a single injection of contrast material. Proc 20th Annual Meeting ISMRM; Melbourne, Australia. 2012. Abstract 524.
18. Maki JH, Wilson GJ, Eubank WB, Hoogeveen RM. Utilizing SENSE to achieve lower station sub-millimeter isotropic resolution and minimal venous enhancement in peripheral MR angiography. J Magn Reson Imaging. 2002; 15(4):484–491. [PubMed: 11948840]
19. Leiner T, Nijenhuis RJ, Maki JH, Lemaire E, Hoogeveen R, van Engelshoven JM. Use of a three-station phased array coil to improve peripheral contrast-enhanced magnetic resonance angiography. J Magn Reson Imaging. 2004; 20(3):417–425. [PubMed: 15332249]
20. Hadizadeh DR, Gieseke J, Lohmaier SH, et al. Peripheral MR angiography with blood pool contrast agent: prospective intraindividual comparative study of high-spatial-resolution steady-state MR angiography versus standard-resolution first-pass MR angiography and DSA. Radiology. 2008; 249(2):701–711. [PubMed: 18769017]
21. Nielsen YW, Eiberg JP, Logager VB, Just S, Schroeder TV, Thomsen HS. Whole-body magnetic resonance angiography with additional steady-state acquisition of the infragenicular arteries in patients with peripheral arterial disease. Cardiovasc Intervent Radiol. 2010; 33(3):484–491. [PubMed: 19957180]
22. Young PM, Mostardi PM, Glockner JF, et al. Prospective comparison of cartesian acquisition with projection-like reconstruction magnetic resonance angiography with computed tomography angiography for evaluation of below-the-knee runoff. J Vasc Interv Radiol. 2013; 24(3):392–399. [PubMed: 23433414]
23. Haider CR, Glockner JF, Stanson AW, Riederer SJ. Peripheral vasculature: high-temporal- and high-spatial-resolution three-dimensional contrast-enhanced MR angiography. Radiology. 2009; 253(3):831–843. [PubMed: 19789238]
24. Hu HH, Campeau NG, Huston J 3rd, Kruger DG, Haider CR, Riederer SJ. High-spatial-resolution contrast-enhanced MR angiography of the intracranial venous system with fourfold accelerated two-dimensional sensitivity encoding. Radiology. 2007; 243(3):853–861. [PubMed: 17446523]
25. Riederer SJ, Hu HH, Kruger DG, Haider CR, Campeau NG, Huston J 3rd. Intrinsic signal amplification in the application of 2D SENSE parallel imaging to 3D contrast-enhanced elliptical centric MRA and MRV. Magn Reson Med. 2007; 58(5):855–864. [PubMed: 17969124]
26. Breuer FA, Blaimer M, Mueller MF, et al. Controlled aliasing in volumetric parallel imaging (2D CAIPIRINHA). Magn Reson Med. 2006; 55(3):549–556. [PubMed: 16408271]
27. Lustig M, Donoho D, Pauly JM. Sparse MRI: The application of compressed sensing for rapid MR imaging. Magn Reson Med. 2007; 58(6):1182–1195. [PubMed: 17969013]
28. Trzasko JD, Haider CR, Borisch EA, et al. Sparse-CAPR: highly accelerated 4D CE-MRA with parallel imaging and nonconvex compressive sensing. Magn Reson Med. 2011; 66(4):1019–1032. [PubMed: 21608028]
29. Weavers PT, Borisch EA, Johnson CP, Riederer SJ. Acceleration apportionment: A method of improved 2D SENSE acceleration applied to 3D contrast-enhanced MR angiography. Magn Reson Med. 2013 epub.
30. Stinson EG, Borisch EA, Johnson CP, Trzasko JD, Young PM, Riederer SJ. Vascular masking for improved unfolding in 2D SENSE-accelerated 3D contrast-enhanced MR angiography. J Magn Reson Imaging. 2013 epub.
31. Kruger DG, Riederer SJ, Grimm RC, Rossman PJ. Continuously moving table data acquisition method for long FOV contrast-enhanced MRA and whole-body MRI. Magn Reson Med. 2002; 47(2):224–231. [PubMed: 11810664]
32. Voth M, Haneder S, Huck K, Gutfleisch A, Schonberg SO, Michaely HJ. Peripheral magnetic resonance angiography with continuous table movement in combination with high spatial and temporal resolution time-resolved MRA with a total single dose (0.1 mmol/kg) of gadobutrol at 3.0 T. Invest Radiol. 2009; 44(9):627–633. [PubMed: 19652610]
33. Leiner T, Habets J, Versluis B, et al. Subtractionless first-pass single contrast medium dose peripheral MR angiography using two-point Dixon fat suppression. Eur Radiol. 2013; 23(8):2228–2235. [PubMed: 23591617]

34. Nikolaou K, Kramer H, Grosse C, et al. High-spatial-resolution multistation MR angiography with parallel imaging and blood pool contrast agent: initial experience. Radiology. 2006; 241(3):861–872. [PubMed: 17032914]

ADVANCES IN KNOWLEDGE

1. A dynamic three-station bolus chase MR angiography method is demonstrated that enables high spatial and temporal resolution imaging of the peripheral arteries while limiting the use of contrast material to a single injection.
2. Fluoroscopic tracking, a method for real-time triggering of table advance, is applied at both proximal stations and effectively eliminates need for a timing bolus.

IMPLICATIONS FOR PATIENT CARE

1. The technique provides high-resolution imaging of the peripheral arteries over an extended field-of-view.
2. The fluoroscopic tracking protocol can potentially reduce total exam time and contrast dose.

SUMMARY STATEMENT

Three-station bolus chase MRA using fluoroscopic tracking provides high-spatial-resolution arteriograms along the extent of the peripheral vasculature, enables patient-specific triggering of table motion, and is a promising alternative to contemporary MRA and CTA methods.

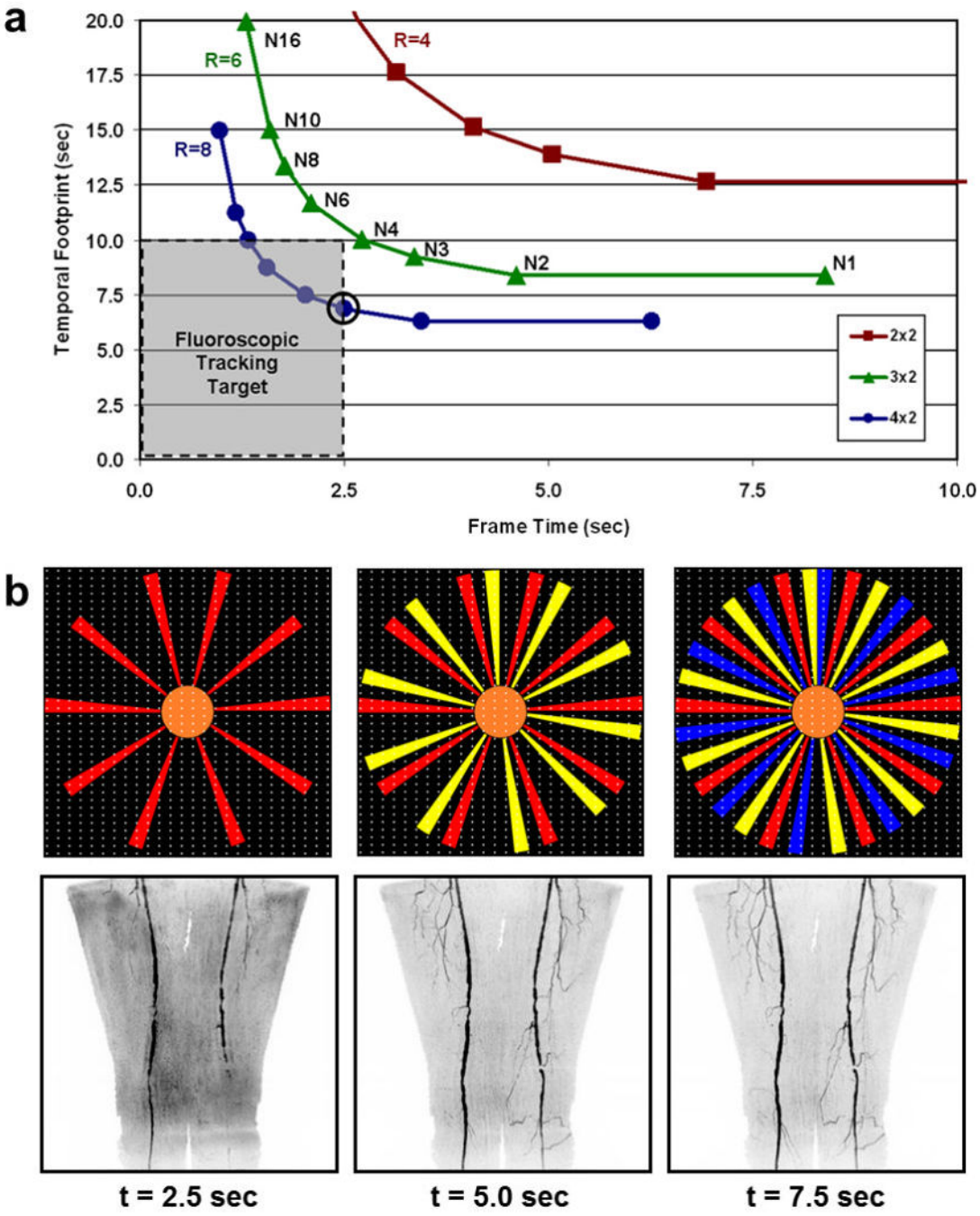

FIGURE 1.

(a) Temporal footprint vs. frame time for CAPR sequences with view share factor N, 2D SENSE acceleration R, and imaging parameters matching those for the abdomen-pelvis station (Table 1). The temporal footprint defines the temporal extent of information required to fully sample the k_Y-k_Z phase encoding plane. For fluoroscopic tracking at the proximal stations, a temporal footprint <10 sec and frame time of 2.5 sec are desired (gray box). An N3 CAPR sequence with R=8 2D SENSE (circled point) meets these targets and was used in this study. **(b)** Temporal filling of the N3 CAPR pattern with sample patient thigh station

time frames from this study (Subject 20) below each phase. During the first 2.5 sec, the center of the k_Y-k_Z phase encoding plane (orange) and one of three highpass vane sets (red) are sampled, producing the first angiogram. During the next 2.5 sec (5.0 sec total), the center is resampled and a second vane set (yellow) is sampled, which quickly builds up vessel signal and sharpness in the second angiogram. The entire k-space is filled after 7.5 sec with sampling of the third vane set (blue).

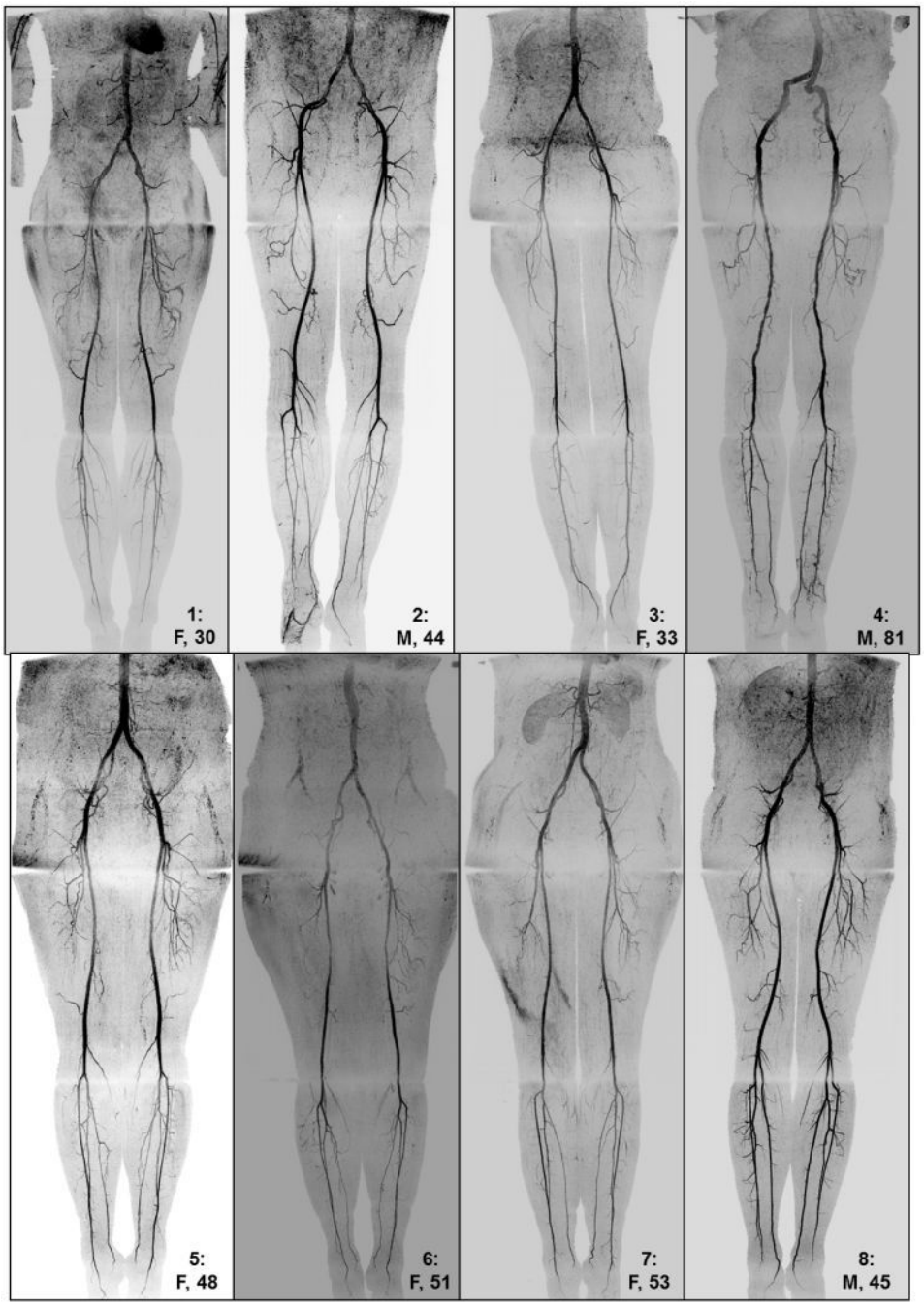

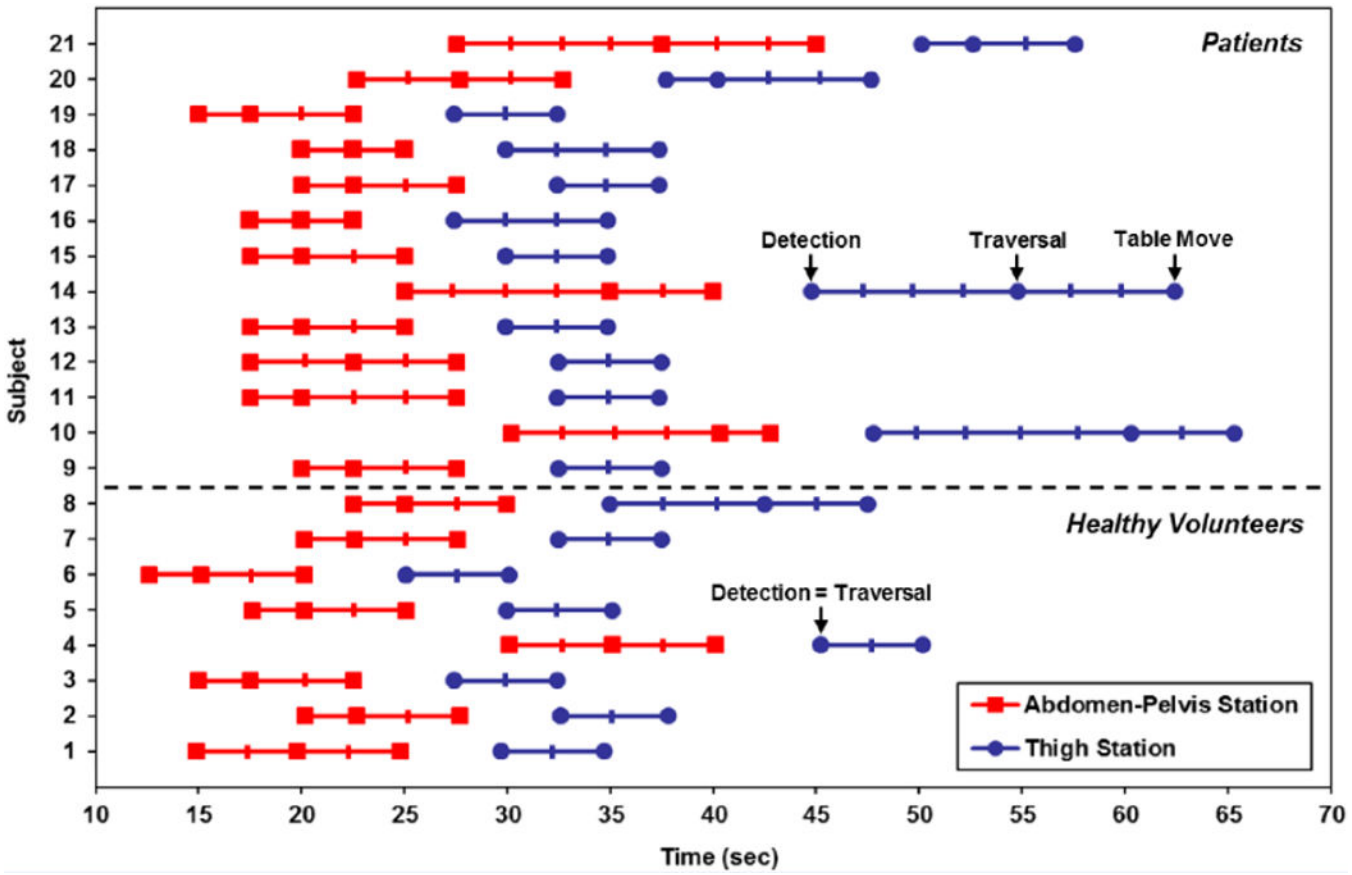

FIGURE 2.

Contrast bolus detection (first marker from left), bolus traversal (second marker), and table move (third marker) times at the abdomen-pelvis (red squares) and thigh (blue circles) stations for all 21 subjects. In many cases the bolus had already traversed the thigh station by the time the acquisition began there, thus the bolus detection and traversal times were the same. Subjects 1–8 are healthy volunteers and Subjects 9–21 are patients. Hash marks indicate fluoroscopic tracking time frame intervals (2.5 sec), and times are relative to the start of contrast material administration.

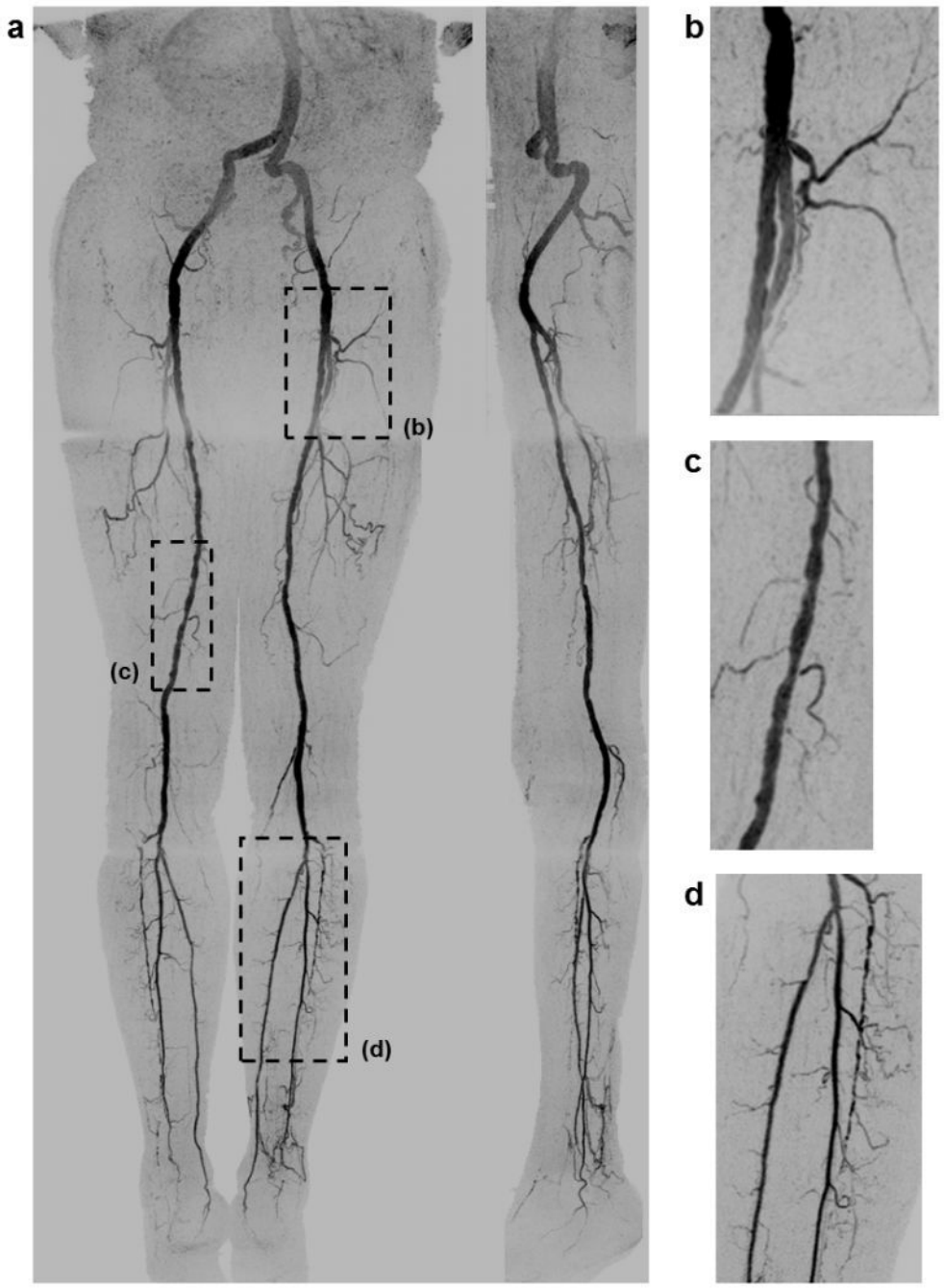

FIGURE 3.

(a) Coronal and sagittal (left leg) MIPs of a healthy 81 year old male volunteer (Subject 4) generated using the final abdomen-pelvis and thigh station time frames and the third calf-foot time frame. The dwell time at the thigh station was only 5.0 sec. Targeted coronal MIPs of the boxed regions in **(a)** are shown in **(b–d)**, highlighting the arterial detail. Although this subject was recruited as a healthy volunteer, multiple low grade stenoses are seen in the thigh and calf arteries, and the anterior tibial arteries are partially occluded. The contrast bolus was imaged at four abdomen-pelvis and two thigh station time frames, and venous

contamination was avoided at the calf-foot station. Reproduced with permission from Ref. (17). Also see Supplemental Figure 1 and Movie 1.

FIGURE 4.

Coronal MIPs of the **(a)** extended FOV and **(b)** calf-foot station of an 81 year old male patient (Subject 10) with slow contrast bolus progression. The transit times at the abdomen-pelvis and thigh proximal stations were 10.0 and 12.5 sec, respectively. The extended FOV angiogram was generated using the last abdomen-pelvis and thigh time frames and the second calf-foot frame. The calf-foot MIP shows the third time frame, which has excellent arterial contrast and detail. The calf vasculature has extensive disease and complex flow, including occlusion of both tibioperoneal trunks and filling of the posterior tibial and

peroneal arteries via communicating vessels. This study was scored substantially better than the CTA due to the CTA outstripping the bolus on the first run and the second run having suboptimal contrast and anatomical coverage. Also see Supplemental Movie 2.

FIGURE 5.

Extended FOV coronal MIP of a 47 year old female patient (Subject 11) with rapid contrast bolus transit. Upon the bolus reaching the distal abdominal aorta, only two additional time frames were acquired at the abdomen-pelvis station, and only two time frames were acquired at the thigh station. However, arterial-to-venous transit was slow at the calf-foot station, thus venous contamination was not seen. The MIP consists of the final abdomen-pelvis and thigh station time frames and the third calf-foot time frame. No preference was given for the MRA vs. the CTA since the CTA allowed better visualization of the left

common iliac stent and left foot vasculature but also exhibited mild venous contamination near the popliteal arteries. Also see Supplemental Movie 3.

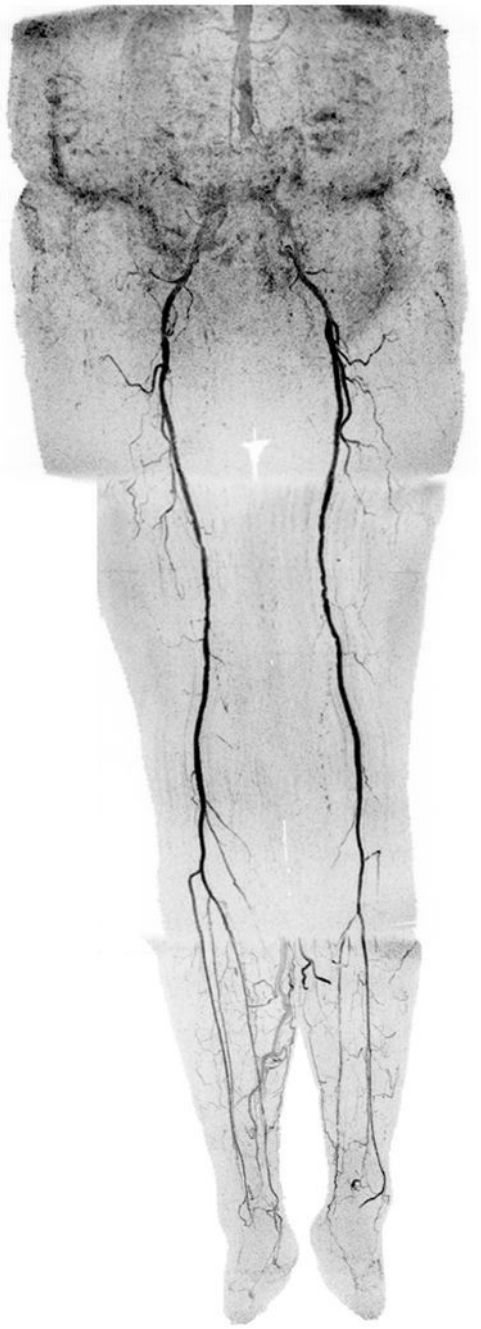

FIGURE 6.

Coronal MIP of a 73 year old female patient (Subject 12) with extensive motion-related artifact at the abdomen-pelvis station and rapid arterial-to-venous transit at the calf-foot station. Due to these effects, the CTA was scored marginally better. The angiogram consists of the final abdomen-pelvis and thigh station time frames and third calf-foot time frame. Also see Supplemental Movie 4.

Table 1

Three-station bolus chase MRA imaging parameters.

	Abdomen-Pelvis	Thighs	Calves-Feet
FOV (cm: S/I × L/R × A/P)	42 × 42 × 14.4	42 × 42 × 13.2	42 × 33.6 × 13.2
Sampling Matrix (S/I × L/R × A/P)	280 × 280 × 96	280 × 280 × 88	420 × 336 × 132
Resolution (mm: S/I × L/R × A/P)	1.5 × 1.5 × 1.5	1.5 × 1.5 × 1.5	1.0 × 1.0 × 1.0
Flip Angle (°)	30	30	30
Bandwidth (kHz)	±62.5	±62.5	±62.5
TR / TE (ms)	4.7 / 2.0	4.7 / 2.0	6.0 / 2.7
Receiver Coils	12–14	10	8
View Sharing Sequence	N3 CAPR	N3 CAPR	N4 CAPR
2D SENSE Acceleration (L/R × A/P)	R=8 (4×2)	R=8 (4×2)	R=8 (4×2)
2D Partial Fourier Acceleration	1.9	1.9	1.8
Frame Time (sec)	2.5	2.5	5.2
Temporal Footprint (sec)	6.9	6.6	18.6

Table 2

Vessel segment image quality assessment scores for both readers in aggregate.

	N		Vessel Signal		Vessel Sharpness		Presence of Artifact		Venous Contamination	
Arterial Segment	**Vol**	**Pt**	**Vol**	**Pt**	**Vol**	**Pt**	**Vol**	**Pt**	**Vol**	**Pt**
Distal Abdominal Aorta	16	26	3.8 (0.9)	3.7 (1.2)	3.9 (0.8)	3.3 (1.1)	3.0 (0.7)	2.6 (0.9)	5.0 (0.0)	5.0 (0.0)
Common Iliac	32	50	3.8 (1.0)	3.3 (1.3)	3.7 (0.8)	3.0 (1.2)	3.3 (0.8)	2.7 (1.0)	5.0 (0.0)	4.8 (0.8)
Internal Iliac	32	52	3.8 (0.8)	3.4 (1.1)	3.8 (0.8)	3.3 (1.0)	3.4 (1.1)	2.8 (1.1)	5.0 (0.0)	4.8 (0.6)
External Iliac	32	49	3.7 (0.6)	3.7 (0.9)	3.7 (0.7)	3.4 (1.0)	3.3 (0.8)	3.0 (1.0)	5.0 (0.0)	4.8 (0.6)
Common Femoral	32	52	4.7 (0.5)	4.4 (0.7)	4.5 (0.7)	4.0 (0.9)	4.3 (0.7)	4.0 (0.9)	5.0 (0.0)	5.0 (0.2)
Superficial Femoral	32	51	4.4 (0.6)	4.5 (1.0)	4.4 (0.8)	4.3 (1.1)	3.9 (0.7)	4.0 (1.1)	5.0 (0.0)	5.0 (0.2)
Deep Femoral	32	52	4.3 (0.7)	4.1 (1.0)	4.4 (0.5)	4.1 (1.0)	4.1 (0.7)	4.0 (1.0)	5.0 (0.0)	5.0 (0.2)
Popliteal	32	50	4.9 (0.3)	4.3 (1.2)	4.8 (0.4)	4.2 (1.2)	4.5 (0.5)	4.0 (1.2)	5.0 (0.0)	4.9 (0.3)
Tibioperoneal Trunk	30	48	4.9 (0.3)	4.3 (1.0)	4.9 (0.4)	4.3 (0.9)	4.5 (0.5)	4.2 (1.0)	4.9 (0.2)	4.6 (0.6)
Proximal Anterior Tibial	32	47	4.9 (0.3)	4.4 (0.8)	4.8 (0.4)	4.4 (0.9)	4.5 (0.6)	4.3 (0.8)	4.9 (0.2)	4.2 (1.1)
Proximal Posterior Tibial	32	46	4.8 (0.6)	4.5 (0.9)	4.8 (0.5)	4.4 (0.9)	4.5 (0.6)	4.2 (0.9)	4.8 (0.4)	4.1 (1.1)
Proximal Peroneal	32	49	4.9 (0.3)	4.5 (0.8)	4.9 (0.3)	4.4 (0.8)	4.5 (0.5)	4.2 (0.8)	4.8 (0.4)	4.0 (1.1)
Distal Anterior Tibial	32	50	4.8 (0.5)	4.3 (1.0)	4.8 (0.4)	4.2 (1.0)	4.6 (0.5)	4.2 (0.8)	4.8 (0.4)	4.1 (1.1)
Distal Posterior Tibial	30	47	4.7 (0.5)	4.5 (0.9)	4.7 (0.4)	4.3 (0.9)	4.5 (0.5)	4.2 (0.9)	4.9 (0.3)	4.1 (1.2)
Distal Peroneal	32	47	4.8 (0.4)	4.4 (0.8)	4.8 (0.4)	4.3 (0.8)	4.5 (0.5)	4.2 (0.8)	4.8 (0.5)	4.0 (1.1)
Dorsalis Pedis	30	45	4.1 (0.9)	4.1 (1.1)	4.1 (0.9)	4.1 (1.1)	4.4 (0.6)	4.1 (0.9)	4.6 (0.8)	4.0 (1.1)
Distal Plantar	28	27	2.9 (1.3)	3.6 (1.0)	3.1 (1.3)	3.8 (0.9)	4.0 (0.7)	3.9 (0.8)	4.5 (0.9)	3.7 (1.1)
Plantar Arch	9	6	3.0 (0.7)	3.7 (2.1)	3.2 (0.4)	3.7 (2.1)	3.4 (0.5)	3.7 (2.1)	4.3 (0.7)	2.7 (1.9)

N is the total number of segments scored in aggregate for healthy volunteers (Vol) and patients (Pt). Scoring was done on a five-point scale (5=best). Reader aggregate scores are reported as: mean (standard deviation).

Table 3

MRA vs. CTA paired comparisons: scores for both readers and N=10 studies.

		−2 = MRA Substantially Better	−1 = MRA Marginally Better	0 = Neutral	+1 = CTA Marginally Better	+2 = CTA Substantially Better	MRA vs CTA Significance
Visualization of Disease	Reader 1	1	3	1	2	3	$p = 0.50$
	Reader 2	0	3	2	4	1	$p = 0.41$
Reading Confidence	Reader 1	1	2	2	2	3	$p = 0.39$
	Reader 2	3	1	2	3	1	$p = 0.61$
Overall Diagnostic Quality	Reader 1	1	2	2	2	3	$p = 0.39$
	Reader 2	0	4	0	4	2	$p = 0.33$

Table 4

Bolus timing assessment mean values and ranges for all N=21 studies.

	Abdomen-Pelvis Station		Thigh Station	
	Mean (Std Dev.)	Min-Max	Mean (Std Dev.)	Min-Max
Bolus Detection (sec)	20.0 (4.8)	12.6 – 30.2	33.9 (7.1)	25.1 – 50.1
Bolus Transit (sec)	4.0 (2.7)	2.5 – 10.1	1.7 (3.7)	0.0 – 12.5
Station Dwell (sec)	8.9 (3.0)	5.0 – 17.5	7.2 (4.0)	5.0 – 17.6
Trigger Delay (sec)	4.9 (1.2)	2.5 – 7.5	5.5 (1.0)	5.0 – 7.6

Bolus Transit is defined as Bolus Traversal – Bolus Detection; Station Dwell is defined as Table Move – Bolus Detection; and Trigger Delay is defined as Table Move – Bolus Traversal.